

Electromagnetic radiation by quark-gluon plasma in magnetic field

Kirill Tuchin¹

¹ *Department of Physics and Astronomy, Iowa State University, Ames, IA 50011*

(Dated: June 15, 2021)

The electromagnetic radiation by quark-gluon plasma in strong magnetic field is calculated. The contributing processes are synchrotron radiation and one-photon annihilation. It is shown that in relativistic heavy-ion collisions at RHIC and LHC synchrotron radiation dominates over the annihilation. Moreover, it constitutes a significant part of all photons produced by the plasma at low transverse momenta; its magnitude depends on the plasma temperature and the magnetic field strength. Electromagnetic radiation in magnetic field is probably the missing piece that resolves a discrepancy between the theoretical models and the experimental data. It is argued that electromagnetic radiation increases with the magnetic field strength and plasma temperature.

I. INTRODUCTION

It has been known for a long time that strong magnetic fields can be generated in heavy-ion collisions. Recent calculations [1–5] confirm this wisdom and predict, using essentially classical electrodynamics, that the magnetic field shortly after the collision reaches $10^{18} - 10^{19}$ G, which by far exceeds the critical value $B_c = 4.41 \cdot 10^{13}$ G for electrons, known also as the Schwinger field. However, it was only recently appreciated that such fields may have great phenomenological significance. There are two observations leading to this conclusion: (i) phenomenological models suggest that the Quark Gluon Plasma (QGP) is formed after a very short time after the heavy-ion collision – on the order of a few tenth of a fm/c; (ii) the relaxation time of magnetic field in the presence of QGP is proportional to the plasma electric conductivity due to the induction of electric Foucault currents by the time-dependent magnetic field [6]. The relaxation time of magnetic field is estimated to be about 1–2 few fm/c [6]. Therefore, magnetic field has a profound influence on all aspects of the physics of relativistic heavy-ion collisions. In particular, it was argued in [6] that magnetic field induces energy loss by fast quarks and charged leptons via the synchrotron radiation and polarization of the fermion spectra. It contributes to enhancement of dilepton production at low invariant masses [7] and enhances the azimuthal anisotropy of the quark-gluon plasma (QGP) [8, 9]. It causes dissociation of the bound states, particularly charmonia, via ionization [10, 11]. Additionally, magnetic field drives the Chiral Magnetic Effect (CME) [1, 12–15], which is the

generation of an electric field parallel to the magnetic one via the axial anomaly in the hot nuclear matter. Additionally, the effect of the magnetic field on the QCD phase diagram was studied using model calculations [16–33] and lattice simulations [33–37]. It is also argued in Appendix, that at RHIC, at early times after heavy ion collision, about 3% of energy density of plasma resides in the magnetic field, while at LHC, this fraction reaches as much as 40%.

This paper addresses the problem of photon radiation by quarks and antiquarks of QGP moving in external magnetic field. This radiation originates from two sources: (i) synchrotron radiation and (ii) quark and antiquark annihilation. QGP is transparent to the emitted electromagnetic radiation because its absorption coefficient is suppressed by α^2 . Thus, QGP is shining in magnetic field. The main goal of this paper is to calculate the spectrum and angular distribution of this radiation. In strong magnetic field it is essential to account for quantization of fermion spectra. Indeed, spacing between the Landau levels is of the order \sqrt{eB} , while their thermal width is of the order T . Spectrum quantization is negligible only if $eB \ll T^2$ which is barely the case at RHIC and certainly not the case at LHC (at least during the first few fm’s of the evolution). Fermion spectrum quantization is important not only for hard and electromagnetic probes but also for the bulk properties of QGP.

The presentation is structured as follows. In Sec. II the spectrum and angular distribution of synchrotron radiation by QGP is calculated in the ideal gas approximation and compared to the experimental data. The results exhibited in Fig. 3,4 indicate that photon radiation in magnetic field gives a significant contribution to the total photon yield. This contribution seems to be large enough to account for the discrepancy between the model calculations assuming no magnetic field and the experimental data at RHIC [38].* Moreover, the electromagnetic radiation rapidly increases with B and T suggesting that it plays even more important role at LHC. In Sec. III the photon spectrum emitted in pair annihilation is calculated and it is shown that it is small as compared to synchrotron contribution. A possible way to ascertain existence of synchrotron radiation is discussed in Sec. IV.

II. SYNCHROTRON RADIATION

Motion of charged fermions in external magnetic field, which we will approximately treat as spatially homogeneous, is quasi-classical in the field direction and quantized in the *reaction plane*,

* Another possible explanation has been recently suggested in [39].

which is perpendicular to the magnetic field and span by the impact parameter and the heavy ion collision axis. In high energy physics one usually distinguishes the *transverse plane*, which is perpendicular to the collision axis and span by the magnetic field and the impact parameter. The notation is adopted in which three-vectors are discriminated by the bold face and their component along the field direction by the plain face. Momentum projections onto the transverse plane are denoted by subscript \perp .

In the configuration space, charged fermions move along spiral trajectories with the symmetry axis aligned with the field direction. Synchrotron radiation is a process of photon γ radiation by a fermion f with electric charge $e_f = z_f e$ in external magnetic field B :

$$f(e_f, j, p) \rightarrow f(e_f, k, q) + \gamma(\mathbf{k}), \quad (1)$$

where \mathbf{k} is the photon momentum, p, q are the momentum components along the magnetic field direction and indices $j, k = 0, 1, 2, \dots$ label the discrete Landau levels in the reaction plane. The Landau levels are given by

$$\varepsilon_j = \sqrt{m^2 + p^2 + 2j e_f B}, \quad \varepsilon_k = \sqrt{m^2 + q^2 + 2k e_f B}, \quad (2)$$

In the constant magnetic field only momentum component along the field direction is conserved. Thus, the conservation laws for synchrotron radiation read

$$\varepsilon_j = \omega + \varepsilon_k, \quad p = q + \omega \cos \theta, \quad (3)$$

where ω is the photon energy and θ is the photon emission angle with respect to the magnetic field. Intensity of the synchrotron radiation was derived in [40]. In [41–44] it was thoroughly investigated as a possible mechanism for γ -ray bursts. In particular, synchrotron radiation in electromagnetic plasmas was calculated. Spectral intensity of angular distribution of synchrotron radiation by a fermion in the j 'th Landau state is given by

$$\frac{dI^j}{d\omega d\Omega} = \sum_f \frac{z_f^2 \alpha}{\pi} \omega^2 \sum_{k=0}^j \Gamma_{jk} \{ |\mathcal{M}_\perp|^2 + |\mathcal{M}_\parallel|^2 \} \delta(\omega - \varepsilon_j + \varepsilon_k) \quad (4)$$

where $\Gamma_{jk} = (1 + \delta_{j0})(1 + \delta_{k0})$ accounts for the double degeneration of all Landau levels except the ground one. The squares of matrix elements \mathcal{M} , which appear in (4), corresponding to photon

polarization perpendicular and parallel to the magnetic field are given by, respectively,

$$4\varepsilon_j\varepsilon_k|\mathcal{M}_\perp|^2 = (\varepsilon_j\varepsilon_k - pq - m^2)[I_{j,k-1}^2 + I_{j-1,k}^2] + 2\sqrt{2je_fB}\sqrt{2ke_fB}[I_{j,k-1}I_{j-1,k}]. \quad (5)$$

$$\begin{aligned} 4\varepsilon_j\varepsilon_k|\mathcal{M}_\parallel|^2 = & \cos^2\theta\{(\varepsilon_j\varepsilon_k - pq - m^2)[I_{j,k-1}^2 + I_{j-1,k}^2] - 2\sqrt{2je_fB}\sqrt{2ke_fB}[I_{j,k-1}I_{j-1,k}]\} \\ & - 2\cos\theta\sin\theta\{p\sqrt{2ke_fB}[I_{j-1,k}I_{j-1,k-1} + I_{j,k-1}I_{j,k}] \\ & + q\sqrt{2je_fB}[I_{j,k}I_{j-1,k} + I_{j-1,k-1}I_{j,k-1}]\} \\ & + \sin^2\theta\{(\varepsilon_j\varepsilon_k + pq - m^2)[I_{j-1,k-1}^2 + I_{j,k}^2] + 2\sqrt{2je_fB}\sqrt{2ke_fB}(I_{j-1,k-1}I_{j,k})\}, \quad (6) \end{aligned}$$

where for $j \geq k$,

$$I_{j,k} \equiv I_{j,k}(x) = (-1)^{j-k} \sqrt{\frac{k!}{j!}} e^{-\frac{x}{2}} x^{\frac{j-k}{2}} L_k^{j-k}(x). \quad (7)$$

and $I_{j,k}(x) = I_{k,j}(x)$ when $k > j$. ($I_{j,-1}$ are identically zero). The functions $L_k^{j-k}(x)$ are the generalized Laguerre polynomials. Their argument is

$$x = \frac{\omega^2}{2e_fB} \sin^2\theta. \quad (8)$$

Angular distribution of radiation is obtained by integrating over the photon energies and remembering that ε_k also depends on ω by virtue of (2) and (3):

$$\frac{dI^j}{d\Omega} = \sum_f \frac{z_f^2\alpha}{\pi} \sum_{k=0}^j \frac{\omega^*(\varepsilon_j - \omega^*)}{\varepsilon_j - p\cos\theta - \omega^*\sin^2\theta} \Gamma_{jk} \{|\mathcal{M}_\perp|^2 + |\mathcal{M}_\parallel|^2\}, \quad (9)$$

where photon energy ω is fixed to be

$$\omega^* = \frac{1}{\sin^2\theta} \left\{ (\varepsilon_j - p\cos\theta) - [(\varepsilon_j - p\cos\theta)^2 - 2e_fB(j-k)\sin^2\theta]^{1/2} \right\}. \quad (10)$$

In the context of heavy-ion collisions the relevant observable is the differential photon spectrum. For ideal plasma in equilibrium each quark flavor gives the following contribution to the photon spectrum:

$$\frac{dN^{\text{synch}}}{dt d\Omega d\omega} = \sum_f \int_{-\infty}^{\infty} dp \frac{e_f B (2N_c) V}{2\pi^2} \sum_{j=0}^{\infty} \sum_{k=0}^j \frac{dI^j}{\omega d\omega d\Omega} (2 - \delta_{j,0}) f(\varepsilon_j) [1 - f(\varepsilon_k)], \quad (11)$$

where $2N_c$ accounts for quarks and antiquarks each of N_c possible colors, and $(2 - \delta_{j,0})$ sums over the initial quark spin. Index f indicates different quark flavors. V stands for the plasma volume. The statistical factor $f(\varepsilon)$ is

$$f(\varepsilon) = \frac{1}{e^{\varepsilon/T} + 1}. \quad (12)$$

The δ -function appearing in (4) can be re-written using (2) and (3) as

$$\delta(\omega - \varepsilon_j + \varepsilon_k) = \sum_{\pm} \frac{\delta(p - p_{\pm}^*)}{\left| \frac{p}{\varepsilon_j} - \frac{q}{\varepsilon_k} \right|}, \quad (13)$$

where

$$p_{\pm}^* = \left\{ \begin{array}{l} \cos \theta (m_j^2 - m_k^2 + \omega^2 \sin^2 \theta) \\ \pm \sqrt{[(m_j + m_k)^2 - \omega^2 \sin^2 \theta][(m_j - m_k)^2 - \omega^2 \sin^2 \theta]} \end{array} \right\} / (2\omega \sin^2 \theta). \quad (14)$$

The following convenient notation was introduced:

$$m_j^2 = m^2 + 2je_f B, \quad m_k^2 = m^2 + 2ke_f B. \quad (15)$$

The physical meaning of (14) is that synchrotron radiation of a photon with energy ω at angle θ by a fermion undergoing transition from j 'th to k 'th Landau level is possible only if the initial quark momentum along the field direction equals p_{\pm}^* .

Another consequence of the conservation laws (3) is that for a given j and k the photon energy cannot exceed a certain maximal value that will be denoted by $\omega_{s,jk}$. Indeed, inspection of (14) reveals that this equation has a real solution only in two cases

$$(i) \ m_j - m_k \geq \omega \sin \theta, \quad \text{or} \quad (ii) \ m_j + m_k \leq \omega \sin \theta. \quad (16)$$

The first case is relevant for the synchrotron radiation while the second one for the one-photon pair annihilation as discussed in the next section. Accordingly, allowed photon energies in the $j \rightarrow k$ transition satisfy

$$\omega \leq \omega_{s,jk} \equiv \frac{m_j - m_k}{\sin \theta} = \frac{\sqrt{m^2 + 2je_f B} - \sqrt{m^2 + 2ke_f B}}{\sin \theta}. \quad (17)$$

No synchrotron radiation is possible for $\omega > \omega_{s,jk}$. In particular, when $j = k$, $\omega_{s,jk} = 0$, i.e. no photon is emitted, which is also evident in (10). The reason is clearly seen in the frame where $p = 0$: since $\varepsilon_j \geq \varepsilon_k$, constraints (2) and (3) hold only if $\omega = 0$.

Substitution of (4) into (11) yields the spectral distribution of the synchrotron radiation rate per unit volume

$$\begin{aligned} \frac{dN^{\text{synch}}}{V dt d\Omega d\omega} &= \sum_f \frac{2N_c z_f^2 \alpha}{\pi^3} e_f B \sum_{j=0}^{\infty} \sum_{k=0}^j \omega (1 + \delta_{k0}) \vartheta(\omega_{s,ij} - \omega) \int dp \sum_{\pm} \frac{\delta(p - p_{\pm}^*)}{\left| \frac{p}{\varepsilon_j} - \frac{q}{\varepsilon_k} \right|} \\ &\quad \times \{ |\mathcal{M}_{\perp}|^2 + |\mathcal{M}_{\parallel}|^2 \} f(\varepsilon_j) [1 - f(\varepsilon_k)], \end{aligned} \quad (18)$$

where ϑ is the step-function.

The natural variables to study the synchrotron radiation are the photon energy ω and its emission angle θ with respect to the magnetic field. However, in high energy physics particle spectra are traditionally presented in terms of rapidity y (which for photons is equivalent to pseudo-rapidity) and transverse momentum k_{\perp} . k_{\perp} is a projection of three-momentum \mathbf{k} onto the transverse plane. These variables are not convenient to study electromagnetic processes in external magnetic field. In particular, they conceal the azimuthal symmetry with respect to the magnetic field direction. To change variables, let z be the collision axis and $\hat{\mathbf{y}}$ be the direction of the magnetic field. In spherical coordinates photon momentum is given by $\mathbf{k} = \omega(\sin \alpha \cos \phi \hat{\mathbf{x}} + \sin \alpha \sin \phi \hat{\mathbf{y}} + \cos \alpha \hat{\mathbf{z}})$, where α and ϕ are the polar and azimuthal angles with respect to z -axis. The plane xz is the reaction plane. By definition, $\hat{\mathbf{k}} \cdot \hat{\mathbf{y}} = \cos \theta$ implying that $\cos \theta = \sin \alpha \sin \phi$. Thus,

$$k_{\perp} = \sqrt{k_x^2 + k_y^2} = \frac{\omega \cos \theta}{\sin \phi}, \quad y = -\ln \tan \frac{\alpha}{2}. \quad (19)$$

The second of these equations is the definition of (pseudo)-rapidity. Inverting (19) yields

$$\omega = k_{\perp} \cosh y, \quad \cos \theta = \frac{\sin \phi}{\cosh y}. \quad (20)$$

Because $dy = dk_z/\omega$ the photon multiplicity in a unit volume per unit time reads

$$\frac{dN^{\text{synch}}}{dV dt d^2 k_{\perp} dy} = \omega \frac{dN^{\text{synch}}}{dV dt d^3 k} = \frac{dN^{\text{synch}}}{dV dt \omega d\omega d\Omega} \quad (21)$$

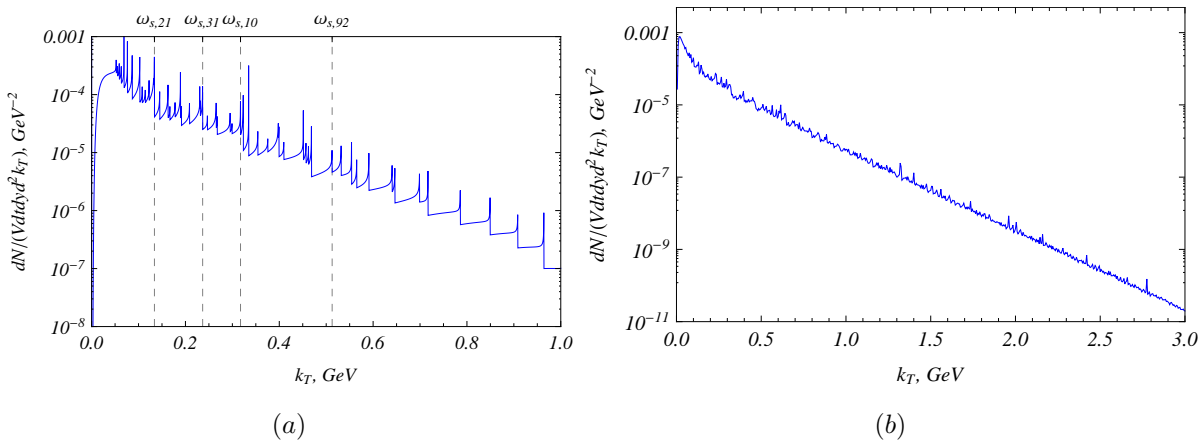


FIG. 1: Spectrum of synchrotron radiation by u quarks at $eB = m_{\pi}^2$, $y = 0$, $\phi = \pi/3$: (a) contribution of 10 lowest Landau levels $j \leq 10$; several cutoff frequencies are indicated; (b) summed over all Landau levels. $m_u = 3$ MeV, $T = 200$ MeV.

Fig. 1 displays the spectrum of synchrotron radiation by u quarks as a function of k_{\perp} at fixed ϕ . At midrapidity $y = 0$ (20) implies that $k_{\perp} = \omega$. Contribution of d and s quarks is qualitatively similar. At $eB \gg m^2$, quark masses do not affect the spectrum much. The main difference

stems from the difference in electric charge. In panel (a) only the contributions of the first ten Landau levels are displayed. The cutoff frequencies $\omega_{s,jk}$ can be clearly seen and some of them are indicated on the plot for convenience. The azimuthal distribution is shown in Fig. 2. Note, that at midrapidity $\phi = \pi/2 - \theta$. Therefore, the figure indicates that photon production in the direction of magnetic field (at $\phi = \pi/2$) is suppressed. More photons are produced in the direction of the reaction plane $\phi = 0$. This results in the ellipticity of the photon spectrum that translates into the positive ‘‘elliptic flow’’ coefficient v_2 . It should be noted, that the classical synchrotron radiation has a similar angular distribution.

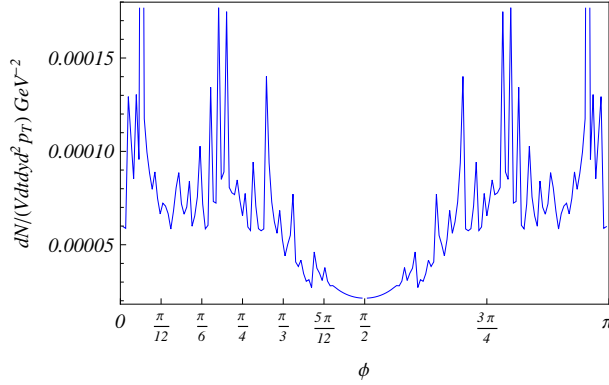


FIG. 2: Azimuthal distribution of synchrotron radiation by u -quarks at $k_{\perp} = 0.2$ GeV, $eB = m_{\pi}^2$, $y = 0$. $m_u = 3$ MeV.

In order to compare the photon spectrum produced by synchrotron radiation to the photon spectrum measured in heavy-ion collisions, the u , d and s quarks contributions were summed up. Furthermore, the experimental data from [38] was divided by Vt , where t is the magnetic field relaxation time. The volume of the plasma can be estimated as $V = \pi R^2 t$ with $R \approx 5$ fm being the nuclear radius. Therefore,

$$\frac{dN_{\text{exp}}^{\gamma}}{dV dt d^2 k_{\perp} dy} = \frac{dN_{\text{exp}}^{\gamma}}{d^2 k_{\perp} dy} \frac{1}{\pi R^2 t^2} = \frac{dN_{\text{exp}}^{\gamma}}{d^2 k_{\perp} dy} \left(\frac{\text{GeV}}{14.9} \right)^4 \left(\frac{1 \text{ fm}}{t} \right)^2. \quad (22)$$

The results are plotted in Fig. 3. In panel (a) it is seen that synchrotron radiation gives a significant contribution to the photon production in heavy-ion collisions at RHIC energy. This contribution is larger at small transverse momenta. This may explain enhancement of photon production observed in [38]. Panel (b) indicates the increase of the photon spectrum produced by the synchrotron radiation mechanism at the LHC energy. This increase is due to enhancement of the magnetic field strength, but mostly because of increase of plasma temperature. This qualitative features can be better understood by considering the limiting cases of low and high photon energies.

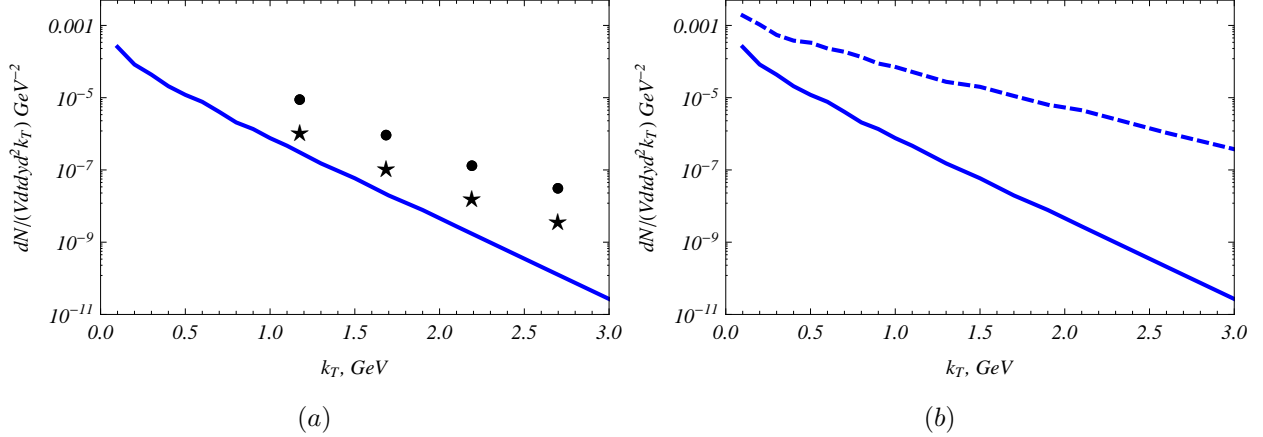


FIG. 3: Azimuthal average of the synchrotron radiation spectrum of u, d, s quarks and their corresponding antiquarks. (a) $eB = m_\pi^2$, $y = 0$ compared to the experimental data from [38] divided by $Vt = 25\pi \text{ fm}^4$ (dots) and $Vt = 9 \times 25\pi \text{ fm}^4$ (stars), (b) $eB = m_\pi^2$, $T = 200 \text{ MeV}$, $y = 0$ (solid line) compared to $eB = 15m_\pi^2$, $T = 400 \text{ MeV}$, $y = 0$ (dashed line). $m_u = 3 \text{ MeV}$, $m_d = 5 \text{ MeV}$, $m_s = 92 \text{ MeV}$.

A. Low photon energy

The low energy part of the photon spectrum satisfies the condition $\omega \ll \sqrt{e_f B}$. The corresponding initial quark momentum component along the field p and energy ε_j follow from (14) and (2) and are given by

$$p_\pm^* \approx \frac{(j-k)e_f B(\cos\theta \pm 1)}{\omega \sin^2\theta} + \mathcal{O}(\omega), \quad \varepsilon_j \approx |p_\pm^*| + \mathcal{O}(\omega). \quad (23)$$

Evidently, $\varepsilon_j \gg eB$. In practice, the magnetic field strength satisfies $\sqrt{e_f B} \gtrsim T$, so that $\varepsilon_j \gg T$. Therefore, synchrotron radiation is dominated by fermion transitions from low Landau levels due to the statistical factors appearing in (11).

For a qualitative discussion it is sufficient to consider the $1 \rightarrow 0$ transition. In this case the matrix elements (5) and (6) read

$$|\mathcal{M}^{1,0}|^2 = \frac{1}{2\varepsilon_1\varepsilon_0} \left\{ I_{1,0}^2(\varepsilon_1\varepsilon_0 - pq \cos^2\theta - m^2) + \cos\theta \sin\theta q \sqrt{2e_f B} I_{1,0} I_{0,0} \right\}. \quad (24)$$

Assuming that the field strength is supercritical, i.e. $e_f B \gg m^2$, but keeping all powers of ω (for future reference) (14) reduces to

$$p_\pm^* \approx \frac{1}{2\omega \sin^2\theta} \left\{ 2e_f B(\cos\theta \pm 1) + \omega^2 \sin^2\theta(\cos\theta \mp 1) \right\}. \quad (25)$$

Furthermore, using the conservation laws (3) we obtain in this approximation

$$\varepsilon_{1\pm} = \frac{1}{2\omega \sin^2 \theta} |2e_f B (\cos \theta \pm 1) - \omega^2 \sin^2 \theta (\cos \theta \mp 1)|, \quad (26)$$

$$q_{\pm} = \frac{1}{2\omega \sin^2 \theta} (2e_f B - \omega^2 \sin^2 \theta) (\cos \theta \pm 1), \quad (27)$$

$$\varepsilon_{0\pm} = |q|. \quad (28)$$

The values of the non-vanishing matrix elements $I_{j,k}$ defined by (7) are

$$I_{1,0}(x) = -x^{1/2} e^{-x/2}, \quad I_{0,0}(x) = e^{-x/2}. \quad (29)$$

For $j = 1$, $k = 0$ we write using (17) $\omega_{s,10} = \sqrt{2e_f B} / \sin \theta$. Then (8) implies $x = \omega^2 / \omega_{s,10}^2$. Substituting (25)–(29) into (24) gives

$$|\mathcal{M}_{\pm}^{1,0}|^2 = \frac{1}{2} x e^{-x} \left[1 - \frac{\cos \theta (1+x) \pm (1-x)}{\cos \theta (1-x) \pm (1+x)} \cos^2 \theta - \frac{2(1-x) \cos \theta \sin^2 \theta}{\cos \theta (1-x) \pm (1+x)} \right]. \quad (30)$$

According to (18) the contribution of the $1 \rightarrow 0$ transition to the synchrotron radiation reads

$$\begin{aligned} \frac{dN^{\text{synch},10}}{V dt d\Omega d\omega} &= \sum_f \frac{2N_c z_f^2 \alpha}{\pi} \omega \Gamma \frac{e_f B}{2\pi^2} \sum_{\pm} f(\varepsilon_1) [1 - f(\varepsilon_0)] |\mathcal{M}_{\pm}^{1,0}|^2 \\ &\quad \times \frac{(1-x) \cos \theta \pm (1+x)}{-2x(\cos \theta \mp 1)} \vartheta(\omega_{s,10} - \omega). \end{aligned} \quad (31)$$

Consider radiation spectrum at $\theta = \pi/2$, i.e. perpendicular to the magnetic field. The spectrum increases with x and reaches maximum at $x = 1$. Since $x = \omega^2 / (2e_f B)$, spectrum decreases with increase of B at fixed ω . This feature holds at low x part of the spectrum for other emission angles and even for transitions from higher excited states. However, at high energies, it is no longer possible to approximate the spectrum by the contribution of a few low Landau levels. In that case the typical values of quantum numbers are $j, k \gg 1$. For example, to achieve the numerical accuracy of 5%, sum over j must run up to a certain j_{max} . Some values of j_{max} are listed in Table I.

B. High photon energy

The high energy tail of the photon spectrum is quasi-classical and approximately continuous. In this case the Laguerre polynomials can be approximated by the Airy functions or the corresponding modified Bessel functions. The angular distribution of the spectrum can be found in [41]:

$$\frac{dN^{\text{synch}}}{V dt d\Omega d\omega} = \sum_f \frac{z_f^2 \alpha}{\pi} \frac{n_f \omega m^2}{4T^3} \sqrt{\frac{e_f B T \sin \theta}{m^3}} e^{-\omega/T}, \quad (32)$$

f	u	u	u	u	u	u	s	u	u	s
eB/m_π^2	1	1	1	1	1	1	1	15	15	15
T , GeV	0.2	0.2	0.2	0.2	0.2	0.2	0.2	0.4	0.4	0.4
ϕ	$\frac{\pi}{3}$	$\frac{\pi}{3}$	$\frac{\pi}{3}$	$\frac{\pi}{3}$	$\frac{\pi}{6}$	$\frac{\pi}{12}$	$\frac{\pi}{3}$	$\frac{\pi}{3}$	$\frac{\pi}{3}$	$\frac{\pi}{3}$
k_\perp , GeV	0.1	1	2	3	1	1	1	1	2	1
x	0.096	9.6	38	86	29	35	19	0.64	2.6	1.3
j_{\max}	30	40	90	150	120	200	90	8	12	16

TABLE I: The upper summation limit in (18) that yields the 5% accuracy. j_{\max} is the highest Landau level of the initial quark that is taken into account at this accuracy. Throughout the table $y = 0$.

provided that $\omega \gg m\sqrt{mT/e_f B \sin\theta}$. Here n_f is number density of flavor f , which is independent of B :

$$n_f = \frac{2 \cdot 2N_c e_f B}{4\pi^2} \sum_{j=0}^{\infty} \int_{-\infty}^{\infty} dp e^{-\varepsilon_j/T} \approx \frac{4N_c}{\pi^2} T^3. \quad (33)$$

Here summation over j was replaced by integration. It follows that this part of the spectrum increases with magnetic field strength as \sqrt{B} and with temperature as $\sqrt{T}e^{-\omega/T}$. Therefore, variation of the spectrum with T is much stronger than with B . The T dependence is shown in Fig. 4.

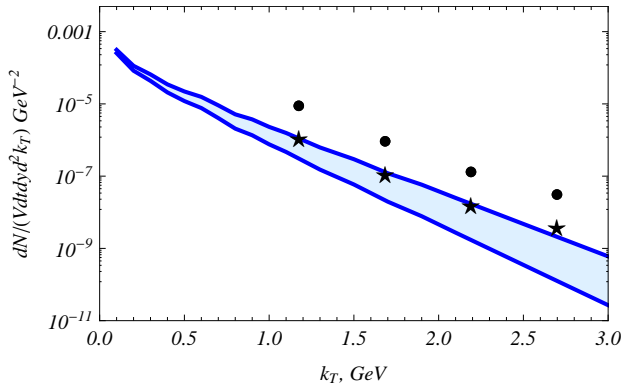


FIG. 4: Variation of the synchrotron spectrum with plasma temperature. Lower line: $T = 200$ MeV, upper line: $T = 250$ MeV. Other parameters are the same as in Fig. 3(a).

III. PAIR ANNIHILATION

The theory of one-photon pair annihilation was developed in [45, 46]. It was shown in [47] that in the super-critical regime $eB \gg m^2$ one-photon annihilations is much larger than the two-photon

annihilation. In this section the one-photon annihilation of q and \bar{q} pairs in the QGP is calculated.

For $q\bar{q}$ pair annihilation the conservation of energy and momentum is given by

$$\varepsilon_j + \varepsilon_k = \omega, \quad p + q = \omega \cos \theta. \quad (34)$$

The spectral density of the annihilation rate per unit volume reads

$$\begin{aligned} \frac{dN^{\text{annih}}}{V dt d\omega d\Omega} &= \sum_f \frac{\alpha z_f^2 \omega N_c}{4\pi e_f B} \sum_{j=0}^{\infty} \sum_{k=0}^{\infty} \int dp \frac{2e_f B}{2\pi^2} f(\varepsilon_j) \int dq \frac{2e_f B}{2\pi^2} f(\varepsilon_k) \\ &\times \delta(p + q - \omega \cos \theta) \delta(\varepsilon_j + \varepsilon_k - \omega) \{ |\mathcal{T}_\perp|^2 + |\mathcal{T}_\parallel|^2 \}, \end{aligned} \quad (35)$$

where the matrix elements \mathcal{T} can be obtained from (5),(6) by making substitutions $\varepsilon_k \rightarrow -\varepsilon_k$, $q \rightarrow -q$ and are given by

$$\begin{aligned} 4\varepsilon_j \varepsilon_k |\mathcal{T}_\perp|^2 &= (\varepsilon_j \varepsilon_k - pq + m^2) [I_{j,k-1}^2 + I_{j-1,k}^2] - 2\sqrt{2je_f B} \sqrt{2ke_f B} [I_{j,k-1} I_{j-1,k}]. \\ 4\varepsilon_j \varepsilon_k |\mathcal{T}_\parallel|^2 &= \cos^2 \theta \{ (\varepsilon_j \varepsilon_k - pq + m^2) [I_{j,k-1}^2 + I_{j-1,k}^2] + 2\sqrt{2je_f B} \sqrt{2ke_f B} [I_{j,k-1} I_{j-1,k}] \} \\ &\quad - 2 \cos \theta \sin \theta \{ -p\sqrt{2ke_f B} [I_{j-1,k} I_{j-1,k-1} + I_{j,k-1} I_{j,k}] \\ &\quad + q\sqrt{2je_f B} [I_{j,k} I_{j-1,k} + I_{j-1,k-1} I_{j,k-1}] \} \\ &\quad + \sin^2 \theta \{ (\varepsilon_j \varepsilon_k + pq + m^2) [I_{j-1,k-1}^2 + I_{j,k}^2] - 2\sqrt{2je_f B} \sqrt{2ke_f B} [I_{j-1,k-1} I_{j,k}] \}, \end{aligned} \quad (36)$$

with the same functions $I_{i,j}$ as in (7). Integration over q removes the delta function responsible for the conservation of momentum along the field direction. The remaining delta function is responsible for energy conservation and can be written in exactly the same form as in (13) with particle energies and momenta now obeying the conservation laws (34). It is straightforward to see that momentum p_\pm^* is still given by (14),(15). The photon spectrum produced by annihilation of quark in state j with antiquark in state k has a threshold $\omega_{a,ij}$ that is given by the case (ii) in (16):

$$\omega \geq \omega_{a,ij} = \frac{m_j + m_k}{\sin \theta} = \frac{\sqrt{m^2 + 2je_f B} + \sqrt{m^2 + 2ke_f B}}{\sin \theta}. \quad (38)$$

Thus, the spectral density of the annihilation rate per unit volume is

$$\begin{aligned} \frac{dN^{\text{annih}}}{V dt d\omega d\Omega} &= \sum_f \frac{\alpha z_f^2 \omega N_c}{4\pi^5} e_f B \sum_{j=0}^{\infty} \sum_{k=0}^{\infty} \vartheta(\omega - \omega_{a,ij}) \int dp \sum_{\pm} \frac{\delta(p - p_\pm^*)}{|\frac{p}{\varepsilon_j} - \frac{q}{\varepsilon_k}|} \\ &\times \{ |\mathcal{T}_\perp|^2 + |\mathcal{T}_\parallel|^2 \} f(\varepsilon_j) f(\varepsilon_k). \end{aligned} \quad (39)$$

Passing to y and p_\perp variables in place of ω and θ is similar to (21).

The results of the numerical calculations are represented in Fig. 5. Panel (a) shows the spectrum of photons radiated in annihilation of u and \bar{u} . We conclude that contribution of the annihilation channel is negligible as compared to the synchrotron radiation.

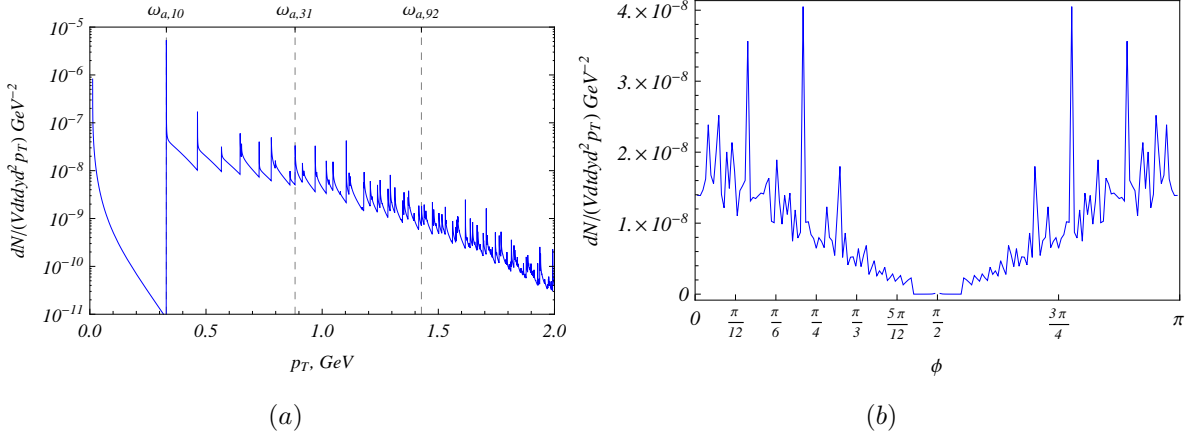


FIG. 5: Photon spectrum in one-photon annihilation of u and \bar{u} quarks. $eB = m_\pi^2$, $y = 0$. (a) k_\perp -spectrum at $\phi = \pi/3$, (b) azimuthal angle distribution at $k_\perp = 1$ GeV.

IV. CONCLUSIONS

Results of the calculations performed in this article indicate that photon production by QGP due to its interaction with external magnetic field give a considerable contribution to the total photon multiplicity in heavy-ion collisions. This is seen in Fig. 3 where the model calculation is compared with the experimental data [38]. The two processes were considered: synchrotron radiation and pair annihilation. In the kinematic region relevant for the current high energy heavy-ion experiments, contribution of the synchrotron radiation is about two orders of magnitude larger than that of pair annihilation. The largest contribution to the photon multiplicity arises from photon momenta of the order of \sqrt{eB} . This may provide an explanation of the photon excess observed by the PHENIX experiment [38]. Similar mechanism is also responsible for enhancement of low mass di-lepton production that proceeds via emission of virtual photon which subsequently decays into di-lepton pair.

One possible way to ascertain the contribution of electromagnetic radiation in external magnetic field is to isolate the azimuthally symmetric component with respect to the direction of the magnetic field. It seems that synchrotron radiation dominates the photon spectrum at low k_\perp . Thus, azimuthal symmetry can be easily checked by simply plotting the multiplicity vs ω , θ and φ , where ω is photon energy, θ is emission angle with respect to the magnetic field and φ is azimuthal angle around the magnetic field direction (which is perpendicular both to the collision axis and to the impact parameter). In Fig. 1(a) it is also seen that in these variables it may be possible to discern the cutoff frequencies $\omega_{s,jk}$ that appear as resonances (in Fig. 1 $y = 0$ so $k_\perp = \omega$). Note that averaging over the azimuthal angle α around the collision axis direction destroys these features, see

Fig. 3.

The greatest source of uncertainty in the present calculation stems from treating the magnetic field as constant. It is inevitable that it has spatial [5] and temporal variations, which will modify the photon spectrum. Analytical calculations of these effects present a serious challenge, but may be tackled in the quasi-classical approximation. Novel computational techniques, such as discussed in [48] is another promising avenue for investigating the particle production in external fields.

Acknowledgments

I thank Yoshimasa Hidaka and Kazunori Itakura for useful correspondence and James Vary for discussions of related topics. This work was supported in part by the U.S. Department of Energy under Grant No. DE-FG02-87ER40371.

Appendix A: Magnetic component of the QGP energy density

Energy density associated with magnetic field is (in Gauss units)

$$\epsilon_M = (eB)^2 / (8\pi\alpha). \quad (\text{A1})$$

Assume that the effect of magnetic field on the QGP is weak and its energy density is much smaller than the total QGP energy density $\epsilon_M \ll \epsilon_{\text{QGP}}$. Then energy density of ideal QGP containing N_f quark flavors at temperature T is given by

$$\epsilon_{\text{QGP}} = \frac{\pi^2}{30} T^4 \left(2(N_c^2 - 1) + \frac{7}{8} 4N_c N_f \right). \quad (\text{A2})$$

With $N_c = 3$, $N_f = 2$ we arrive at the following ratio

$$\frac{\epsilon_M}{\epsilon_{\text{QGP}}} = 0.45 \frac{(eB)^2}{T^4}. \quad (\text{A3})$$

At RHIC $eB \sim m_\pi^2$ and $T \sim 2m_\pi$, so that at early times about 3% of energy density of plasma resides in the magnetic field. At LHC, $eB \sim 15m_\pi^2$ and $T \sim 4m_\pi$ so that as much as 40% is stored in magnetic field! This signals that magnetic field plays a crucial role in QGP dynamics at LHC energies.

[1] D. E. Kharzeev, L. D. McLerran and H. J. Warringa, Nucl. Phys. A **803**, 227 (2008) [arXiv:0711.0950 [hep-ph]].

- [2] V. Skokov, A. Y. Illarionov and V. Toneev, *Int. J. Mod. Phys. A* **24**, 5925 (2009) [arXiv:0907.1396 [nucl-th]].
- [3] V. Voronyuk, V. D. Toneev, W. Cassing, E. L. Bratkovskaya, V. P. Konchakovski, S. A. Voloshin, *Phys. Rev.* **C83**, 054911 (2011). [arXiv:1103.4239 [nucl-th]].
- [4] W. -T. Deng and X. -G. Huang, *Phys. Rev. C* **85**, 044907 (2012) [arXiv:1201.5108 [nucl-th]].
- [5] A. Bzdak and V. Skokov, *Phys. Lett. B* **710**, 171 (2012) [arXiv:1111.1949 [hep-ph]].
- [6] K. Tuchin, *Phys. Rev. C* **82**, 034904 (2010) [Erratum-ibid. *C* **83**, 039903 (2011)] [arXiv:1006.3051 [nucl-th]].
- [7] K. Tuchin, *Phys. Rev.* **C83**, 017901 (2011). [arXiv:1008.1604 [nucl-th]].
- [8] R. K. Mohapatra, P. S. Saumia and A. M. Srivastava, arXiv:1102.3819 [hep-ph].
- [9] K. Tuchin, *J. Phys. G* **39**, 025010 (2012) [arXiv:1108.4394 [nucl-th]].
- [10] K. Marasinghe, K. Tuchin, [arXiv:1103.1329 [hep-ph]].
- [11] K. Tuchin, arXiv:1105.5360 [nucl-th].
- [12] D. Kharzeev, *Phys. Lett.* **B633**, 260-264 (2006). [arXiv:hep-ph/0406125 [hep-ph]].
- [13] D. Kharzeev, A. Zhitnitsky, *Nucl. Phys.* **A797**, 67-79 (2007). [arXiv:0706.1026 [hep-ph]].
- [14] K. Fukushima, D. E. Kharzeev, H. J. Warringa, *Phys. Rev.* **D78**, 074033 (2008). [arXiv:0808.3382 [hep-ph]].
- [15] D. E. Kharzeev, *Annals Phys.* **325**, 205-218 (2010). [arXiv:0911.3715 [hep-ph]].
- [16] A. J. Mizher, M. N. Chernodub and E. S. Fraga, *Phys. Rev. D* **82**, 105016 (2010) [arXiv:1004.2712 [hep-ph]].
- [17] E. S. Fraga and A. J. Mizher, *Nucl. Phys. A* **820**, 103C (2009) [arXiv:0810.3693 [hep-ph]].
- [18] R. Gatto and M. Ruggieri, *Phys. Rev. D* **83**, 034016 (2011) [arXiv:1012.1291 [hep-ph]].
- [19] R. Gatto and M. Ruggieri, *Phys. Rev. D* **82**, 054027 (2010) [arXiv:1007.0790 [hep-ph]].
- [20] A. A. Osipov, B. Hiller, A. H. Blin and J. da Providencia, *Phys. Lett. B* **650**, 262 (2007) [hep-ph/0701090].
- [21] K. Kashiwa, *Phys. Rev. D* **83**, 117901 (2011) [arXiv:1104.5167 [hep-ph]].
- [22] C. V. Johnson and A. Kundu, *JHEP* **0812**, 053 (2008) [arXiv:0803.0038 [hep-th]].
- [23] S. Kanemura, H. -T. Sato and H. Tochimura, *Nucl. Phys. B* **517**, 567 (1998) [hep-ph/9707285].
- [24] J. Alexandre, K. Farakos and G. Koutsoumbas, *Phys. Rev. D* **63**, 065015 (2001) [hep-th/0010211].
- [25] N. O. Agasian and S. M. Fedorov, *Phys. Lett. B* **663**, 445 (2008) [arXiv:0803.3156 [hep-ph]].
- [26] F. Preis, A. Rebhan and A. Schmitt, *JHEP* **1103**, 033 (2011) [arXiv:1012.4785 [hep-th]].
- [27] V. P. Gusynin, V. A. Miransky and I. A. Shovkovy, *Nucl. Phys. B* **462**, 249 (1996) [hep-ph/9509320].
- [28] V. A. Miransky and I. A. Shovkovy, *Phys. Rev. D* **66**, 045006 (2002) [hep-ph/0205348].
- [29] J. K. Boomsma and D. Boer, *Phys. Rev. D* **81**, 074005 (2010) [arXiv:0911.2164 [hep-ph]].
- [30] I. A. Shushpanov and A. V. Smilga, *Phys. Lett. B* **402**, 351 (1997) [hep-ph/9703201].
- [31] T. D. Cohen, D. A. McGady and E. S. Werbos, *Phys. Rev. C* **76**, 055201 (2007) [arXiv:0706.3208 [hep-ph]].

- [32] N. O. Agasian, Phys. Atom. Nucl. **64**, 554 (2001) [Yad. Fiz. **64**, 608 (2001)] [hep-ph/0112341].
- [33] M. D’Elia, S. Mukherjee and F. Sanfilippo, Phys. Rev. D **82**, 051501 (2010) [arXiv:1005.5365 [hep-lat]].
- [34] P. Cea and L. Cosmai, JHEP **0508**, 079 (2005) [hep-lat/0505007].
- [35] P. Cea and L. Cosmai, JHEP **0302**, 031 (2003) [arXiv:hep-lat/0204023].
- [36] P. Cea, L. Cosmai and M. D’Elia, JHEP **0712**, 097 (2007) [arXiv:0707.1149 [hep-lat]].
- [37] G. S. Bali, F. Bruckmann, G. Endrodi, Z. Fodor, S. D. Katz, S. Krieg, A. Schafer and K. K. Szabo, JHEP **1202**, 044 (2012) [arXiv:1111.4956 [hep-lat]].
- [38] A. Adare *et al.* [PHENIX Collaboration], Phys. Rev. Lett. **104**, 132301 (2010) [arXiv:0804.4168 [nucl-ex]].
- [39] M. Chiu, T. K. Hemmick, V. Khachatryan, A. Leonidov, J. Liao and L. McLerran, arXiv:1202.3679 [nucl-th].
- [40] A. A. Sokolov and I. M. Ternov, “*Synchrotron radiation*”, Pergamon Press, Oxford, (1968).
- [41] M. G. Baring, Mon. Not. R. ast. Soc. **235**, 57, (1988).
- [42] H. Herold, H. Ruder and G. Wunner, Astron. Astrophys. **115**, 90, (1982).
- [43] A. K. Harding and R. Preece, Ap. J. **319**, 939, (1987).
- [44] H. G. Latal, Ap. J. **309**, 372, (1986).
- [45] A. K. Harding, Ap. J. **300**, 167, (1986).
- [46] G. Wunner, J. Paez, H. Herold and H. Ruder, Astron. Astrophys. **170**, 179, (1986)
- [47] G. Wunner, Phys. Rev. Lett. **42**, 79, (1979).
- [48] X. Zhao, H. Honkanen, P. Maris, J. P. Vary and S. J. Brodsky, Few Body Syst. **52**, 339 (2012) [arXiv:1110.0553 [hep-ph]].